Nonlinear birefringence and time-resolved Kerr measurement of spin lifetimes in (110) GaAs/$Al_yGa_{1-y}As$ quantum wells

P. S. Eldridge,[1] P. G. Lagoudakis,[1] M. Henini,[2] and R. T. Harley[1]
[1]*School of Physics and Astronomy, University of Southampton, Southampton SO17 1BJ, United Kingdom*
[2]*School of Physics and Astronomy, University of Nottingham, Nottingham NG7 4RD, United Kingdom*
(Received 8 October 2009; revised manuscript received 24 November 2009; published 7 January 2010)

We report a study of the nonlinear birefringence in undoped (110)-oriented GaAs/AlGaAs quantum wells using time-resolved pump-probe Kerr spectroscopy. Due to the optical anisotropy of the (110) quantum well plane, photoexcited carriers can give rise to a nonlinear birefringence and so cause probe polarization rotation independent of the pump polarization, i.e., independent of spin orientation. We develop a methodology for accurate determination of electron-spin lifetimes using the Kerr technique which takes account of this phenomenon and present room-temperature measurements of wavelength and power density dependence of the spin-relaxation rate.

DOI: 10.1103/PhysRevB.81.033302 PACS number(s): 72.25.Fe, 72.25.Rb, 73.21.Fg

I. INTRODUCTION

GaAs quantum wells grown on (110) substrates provide an attractive medium to study electron-spin dynamics as measured electron-spin lifetimes approach those in silicon at room temperature and they allow separation of bulk (bulk inversion asymmetry, BIA) and Rashba (structural inversion asymmetry, SIA) components of the Dyakonov-Perel spin-relaxation mechanism.[1–4] Time-resolved optical Faraday (transmission)[5] and Kerr (reflection)[6] techniques in which a spin-polarized photoexcited carrier population is generated by a circularly polarized pump pulse and monitored through rotation of the plane of a linearly polarized probe pulse are standard techniques used for measuring electron-spin dynamics in quantum wells. They were initially developed for measurements on heterostructures grown on (100) zincblende substrates where the crystal lattice along the growth direction possesses fourfold symmetry and is therefore optically isotropic. In this case the probe rotation is proportional to the difference between spin-up and spin-down photoexcited populations and can be used to monitor directly the spin dynamics. By contrast (110)-oriented quantum wells have twofold in-plane symmetry and are optically birefringent.[7] Therefore, in principle, a photoexcited population will cause a change in the birefringence and a consequent pump-induced rotation of the probe polarization that is independent of spin orientation. This is additional to any rotation due to spin alignment of the photoexcited carriers and so will complicate investigations of spin dynamics.

In this Brief Report we present a study of time-resolved and spectrally resolved Kerr rotation measurements in (110) GaAs/AlGaAs quantum wells. The spectrally resolved measurements reveal the expected spin-independent rotation of the probe while the time-resolved measurements show that it decays at the same rate as the photoexcited population. Accurate spin-relaxation measurements can be obtained by combining measurements taken with opposite circular pump polarizations.

II. EXPERIMENTAL DETAILS

Two undoped GaAs/AlGaAs multiple quantum well samples were studied. They were grown by molecular beam epitaxy on semi-insulating (110)-oriented substrates and had well widths, measured using photoluminescence, of 7.5 nm (sample NU2284) and 5.0 nm (sample NU2572). Each contained 20 GaAs quantum wells with 12 nm $Al_{0.4}Ga_{0.6}As$ barriers. The natural cleavage of the (110)-oriented wafers along [001], $[\bar{1}11]$, and $[1\bar{1}1]$ directions was used to determine the orientation of the principle axes in the well planes, namely, [001] and $[1\bar{1}0]$.

Our pump-probe time-resolved Kerr rotation setup is described in Ref. 8. The train of pulses of ~2 ps duration from a modelocked Ti:Sapphire laser with repetition rate of 76 MHz was split into wavelength-degenerate pump and probe beams. The pump was circularly polarized and thus injected spin-polarized carriers (at time $t=0$). The linearly polarized probe was used to monitor the temporal evolution of this population for increasing delay ($t>0$) by measurement of the pump-induced polarization rotation ($\Delta\theta$) and the intensity change (ΔR) in the reflected probe using balanced detectors. The samples were held at room temperature (~300 K) and the laser was tuned to the region of the $n=1$ heavy-hole exciton line of the quantum wells as indicated by photoluminescence [see Fig. 1(a)]. It has been demonstrated[9] that under these conditions the signals result primarily from phase-space filling by the photoexcited carriers; excitons dissociate into free carriers on a sub-picosecond time scale and as spin relaxation of holes is rapid,[10] any remaining spin alignment on a picosecond time scale can be attributed to the free electrons.

III. RESULTS AND DISCUSSION

For spectrally resolved measurements, the laser wavelength was scanned with the probe delay fixed at 30 ps. Figure 1 shows an example of the measured variation in ΔR and $\Delta\theta$ for sample NU2284 as a function of wavelength for two opposite circular polarizations of the pump ($\sigma^{\pm}$). In this case the probe polarization is set at 47° to [001]. The two ΔR signals [Fig. 1(b)] are almost identical as expected since the number of photoexcited carriers does not depend on the handedness of the pump. The two $\Delta\theta$ signals [Fig. 1(c)] are

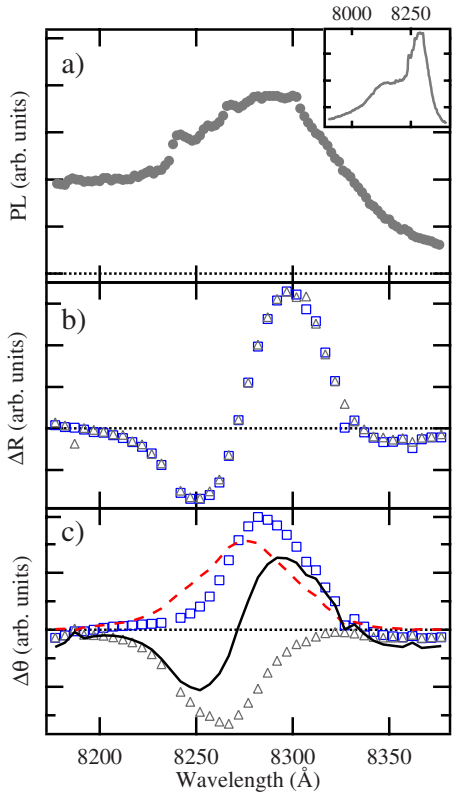

FIG. 1. (Color online) Room-temperature variation with wavelength of (a) photoluminescence near the $n=1$ heavy-hole exciton line (inset shows the spectrum over a wider wavelength range including the $n=1$ light hole exciton line). (b) and (c) probe reflection, $\Delta R^{\pm}$, and polarization rotation, $\Delta\theta^{\pm}$, for σ^{+} (squares) and σ^{-} (triangles) pump polarizations. The pump-probe delay is set at 30 ps and the probe polarization is at 47° to [001] in the well plane. In (c) the solid curve indicates the sum, $(\Delta\theta^{+}+\Delta\theta^{-})$, and the dashed curve half the difference, $(\Delta\theta^{+}-\Delta\theta^{-})/2$.

clearly not equal and opposite, as would be expected if they were due purely to opposite spin alignments. The sum of the two measurements $(\Delta\theta^{+}+\Delta\theta^{-})$, which represents a spin-independent rotation of the probe, is shown by the solid curve in Fig. 1(c). It bears a strong resemblance to the ΔR signal [Fig. 1(b)] as would be expected for rotation resulting from pump-induced nonlinear birefringence. The dashed curve in Fig. 1(c) shows the difference of the two signals $(\Delta\theta^{+}-\Delta\theta^{-})/2$ which indicates the spin-dependent component of the rotation.

Rotation due to nonlinear birefringence should vanish and change sign when the probe polarization coincides with either of the principal axes [001] or $[1\bar{1}0]$. Figure 2 illustrates the verification of this behavior. For a series of angles of the probe with respect to [001], the function $\alpha(\Delta\theta^{+}+\Delta\theta^{-})+\beta$ was fitted to ΔR by adjusting the parameters α (amplitude) and β (offset). Figure 2(a) is a contour plot of the sum of the absolute values of the residuals for an angle of 47°. The best fit corresponds to the minimum at the center of the dark region (red online) and is shown as the curve in Fig. 2(b). At other angles the best fit was similar. Figure 2(c) shows the best-fit values of $1/\alpha$ as a function of angle, demonstrating that indeed the spin-independent probe rotation is zero when

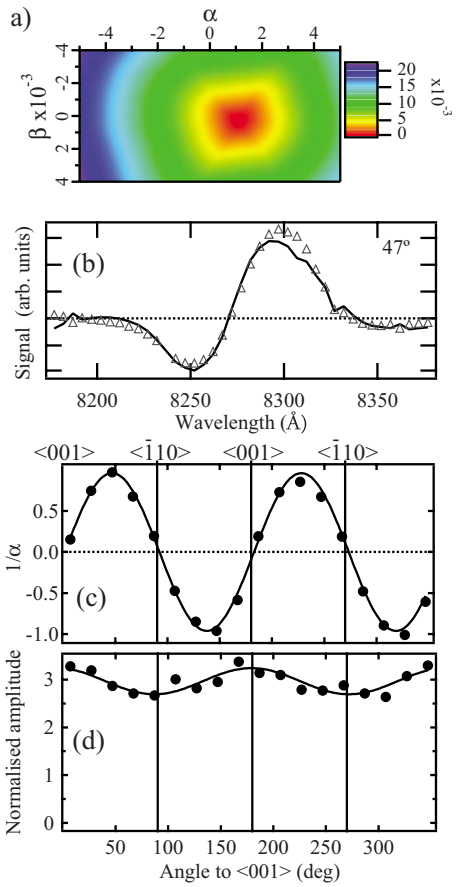

FIG. 2. (Color online) (a)–(c) Fitting the function $\alpha(\Delta\theta^{+}+\Delta\theta^{-})+\beta$ to ΔR with α and β as parameters. (a) Contour plot of the sum of the absolute values of residuals for probe polarization at 47° to [001]; best fit corresponds to center of dark region (red in color). (b) The resulting best-fit solid curve to data for ΔR (triangles). (c) Values of $1/\alpha$ for different angles of the probe polarization. (d) The angular dependence of the maximum amplitude of $(\Delta\theta^{+}-\Delta\theta^{-})$ normalized by the amplitude of $(\Delta R^{+}+\Delta R^{-})$. Curves in (c) and (d) are sinusoidal fits to the data.

the probe polarization coincides with either of the principal axes in the well plane. Figure 2(d) shows the angular dependence of the amplitude of the difference of the two rotation signals $(\Delta\theta^{+}-\Delta\theta^{-})$ which represents the spin-dependent rotation. The raw data at each angle have been normalized to the average amplitude of the ΔR^{+} and ΔR^{-} signals [see Fig. 1(b)] in order to remove effects of other experimental parameters that affect the signal. In contrast to the spin-independent component, this spin-dependent rotation is almost isotropic showing only a small variation of twofold symmetry with maxima along [001]. Similar results were obtained for sample NU2572.

Next we investigate the time dependence of the Kerr rotation signals. Figure 3(a) shows the time evolution of the ΔR signal for two opposite circular pump polarizations and also of $(\Delta\theta^{+}+\Delta\theta^{-})$ each recorded for probe polarization at 45° to $[\bar{1}10]$. It is clear that the decay rates of the three signals are approximately equal, confirming that the spin-independent rotation signal follows the photoexcited population. Figure 3(b) compares the time evolution of the $\Delta\theta^{+}$

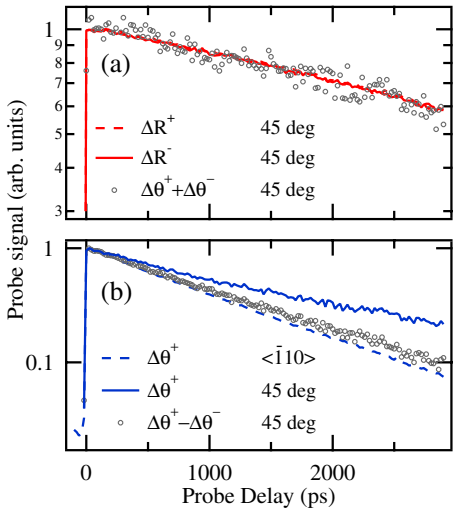

FIG. 3. (Color online) (a) Comparison of temporal evolution of the $\Delta R^{\pm}$ signals (dashed and solid curves) with that of the spin-independent rotation signal $(\Delta\theta^{+}+\Delta\theta^{-})$ (points) for probe polarization at 45° to $[\bar{1}10]$. (b) Evolution of $\Delta\theta^{+}$ for probe polarization parallel to and at 45° to $[\bar{1}10]$ (dashed and solid curves, respectively) compared to that of the spin-dependent rotation signal $(\Delta\theta^{+}-\Delta\theta^{-})$ (points).

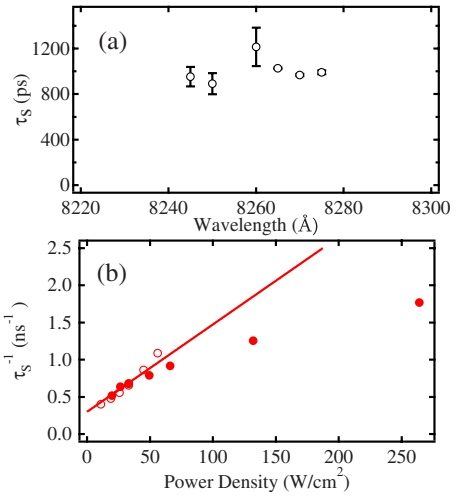

FIG. 4. (Color online) (a) Measured spin lifetimes at different energies. (b) The power dependence of the spin-relaxation rate in NU2284 (solid circles). Open circles are data from Ref. 11.

signal for probe polarization along $[\bar{1}10]$ where the spin-independent signal is very small [see Fig. 2(c)] with $(\Delta\theta^{+}-\Delta\theta^{-})$ measured for probe at 45° to $[\bar{1}10]$. These two decays are nearly equal and show a rate considerably faster than that of the ΔR signal [Fig. 3(a)] which is consistent with the additional effect of spin relaxation. Figure 3(b) also shows the decay of the $\Delta\theta^{+}$ signal for probe at 45° to $[\bar{1}10]$. There is a slower and nonexponential decay consistent with the combination of spin-dependent and spin-independent rotational signals.

Clearly to eliminate effects of the spin-independent Kerr rotation due to nonlinear pump-induced birefringence it is necessary to orient the probe polarization along one of the principal axes in the well plane $[\bar{1}10]$ or [001] and to record the difference of rotations for the two opposite circular pump polarizations. The electron-spin-relaxation rate can be extracted by taking the difference of the decay rates for the combinations $(\Delta\theta^{+}-\Delta\theta^{-})$ and $(\Delta R^{+}+\Delta R^{-})$.

With these precautions we show in Fig. 4(a) the dependence on wavelength of the extracted spin-relaxation time for sample NU2284; within experimental uncertainties the time is independent of wavelength. Figure 4(b) shows the pump-power density dependence of the spin-relaxation rate also for sample NU2284. For comparison we include measurements on a sample with similar quantum well width made by Ohno *et al.*[11] using the Faraday rotation technique. At low powers both data sets follow a linear relationship, while at higher powers the relationship becomes sublinear. The linear increase in the spin-relaxation rate with power density is consistent with spin lifetimes being limited by the Bir-Aronov-Pikus (BAP) spin-relaxation mechanism,[12] in which electron-spin orientation is lost via the exchange interaction with unpolarized holes. This is an intrinsic mechanism and the agreement at low power between the two samples from completely different sources provides further support for the importance of the BAP mechanism in (110) quantum wells. Possible explanations of the observed saturation at high-power densities are screening of the electron-hole exchange interaction or heating of the electron-hole plasma making the BAP mechanism less effective. The extrapolated spin-relaxation time at zero carrier density is 4 ns.

ACKNOWLEDGMENT

We acknowledge EPSRC for financial support.

[1] T. Adachi, Y. Ohno, F. Matsukura, and H. Ohno, Physica E (Amsterdam) **10**, 36 (2001).
[2] B. Huang, D. J. Monsma, and I. Appelbaum, Phys. Rev. Lett. **99**, 177209 (2007).
[3] O. Z. Karimov, G. H. John, R. T. Harley, W. H. Lau, M. E. Flatte, M. Henini, and R. Airey, Phys. Rev. Lett. **91**, 246601 (2003).
[4] P. S. Eldridge, W. J. H. Leyland, P. G. Lagoudakis, O. Z. Karimov, M. Henini, D. Taylor, R. T. Phillips, and R. T. Harley, Phys. Rev. B **77**, 125344 (2008).
[5] J. J. Baumberg, D. D. Awschalom, N. Samarth, H. Luo, and J. K. Furdyna, Phys. Rev. Lett. **72**, 717 (1994).
[6] N. I. Zheludev, M. A. Brummell, R. T. Harley, A. Malinowski, S. V. Popov, D. E. Ashenford, and B. Lunn, Solid State Commun. **89**, 823 (1994).
[7] D. Gershoni, I. Brener, G. A. Baraff, S. N. G. Chu, L. N. Pfeiffer,

and K. West, Phys. Rev. B **44**, 1930 (1991).
[8] R. T. Harley, O. Z. Karimov, and M. Henini, J. Phys. D **36**, 2198 (2003).
[9] M. J. Snelling, P. Perozzo, D. C. Hutchings, I. Galbraith, and A. Miller, Phys. Rev. B **49**, 17160 (1994).
[10] B. Baylac, T. Amand, X. Marie, B. Dareys, M. Brousseau, G. Bacquet, and V. Thierrymieg, Solid State Commun. **93**, 57 (1995).
[11] Y. Ohno, R. Terauchi, T. Adachi, F. Matsukura, and H. Ohno, Phys. Rev. Lett. **83**, 4196 (1999).
[12] G. L. Bir, A. G. Aronov, and G. E. Pikus, Zh. Eksp. Teor. Fiz. Pis'ma Red. **69**, 1382 (1975) [Sov. Phys. JETP **42**, 705 (1976)].